ESA Contract Report

ESA 4000130590/20/NL/IA

Contract Report to the European Space Agency

WP-1000 Review of EDA approach and recommendations for small satellite configurations

Technical Note 1 (final version) for ESA contract no. 4000130590/20/NL/IA

Authors: Katie Lean, Niels Bormann and Sean Healy

January 2021

Series: ECMWF ESA Contract Report Series

A full list of ECMWF Publications can be found on our web site under:
http://www.ecmwf.int/en/publications/

Contact: library@ecmwf.int

European Centre for Medium Range Weather Forecasts, Shinfield Park, Reading, RG2 9AX, UK

Contents

1 Introduction

The start of October 2020 marked the beginning of a project to investigate potential future constellations of small satellites carrying microwave (MW) sounding instruments. Observations from MW instruments currently provide the greatest impact of the satellite data used in the ECMWF assimilation system (Bormann et al., 2019). We are currently in a fortunate era of having nine and eleven MW instruments with temperature and humidity sounding capabilities respectively in operational use from a variety of polar orbiting platforms. Continued positive impact is still found from the latest additional sounders showing that a saturation point, where new data brings no significant benefit, has not yet been reached (Duncan and Bormann, 2020). This prompts the question of how much further benefit could be achieved with even better temporal sampling from additional instruments. At the same time, many of these satellites are well past their design-life or will be decommissioned in coming years, with only a few new MW sounding instruments scheduled for launch. So in the immediate future, the constellation as it stands now is expected to decline in the coming years.

Recent advances in technology have allowed the possibility of launching MW sounding instruments on small satellites with a performance that is expected to be adequate for Numerical Weather Prediction (NWP). While some compromises remain with the compact instruments, such as the potential loss of lower frequency wavelengths (below 50GHz) or marginally poorer noise performance, the small satellites provide a cost-effective means to enhance the temporal sampling provided from MW sounding instruments. Such constellations are expected to become an important presence in the future observing system, as a complement to fully specified instruments on a back-bone constellation of larger platforms. The higher temporal sampling will allow us to better observe faster evolving cloud and humidity features and to reduce the random component of noise through higher measurement numbers.

This project will consider various options for a possible new constellation of small satellites in order to make recommendations for the design that balance the benefit to NWP with practicalities such instrument limitations and cost. Key questions to consider include:

- What is the optimal number of satellites and their orbit type (e.g. polar or low inclination orbits)?
- What sets of channels (humidity and/or temperature sounding) provide the most benefit?
- What are the effects from limitations in performance and geo-location accuracy?

The benefit to NWP of different configurations of small satellites carrying MW sounding instruments will be assessed using an Ensemble of Data Assimilations (EDA) method. EDA experiments concerning simulated satellite data have recently been used at ECMWF to evaluate the impact of increasing numbers of Global Navigation Satellite System (GNSS) Radio Occultation (RO) observations (Harnisch et al., 2013) and the benefit from Aeolus (Tan et al., 2007).

In this report we will start by providing a short description of the EDA method (section 2) and review the planned approach for this project, considering the experience from previous studies (section 3). This includes considering the required length of study period and necessary adaptations for the observation error modelling. Section 3.3 considers the key themes we would like to address concluding with an initial recommendation of a list of scenarios. The exact list of parameters required from ESA as part of the data simulation step is given in Appendix B.

2 Use of the EDA to assess observation impact

2.1 Methodology of the Ensemble of Data Assimilations

The Ensemble of Data Assimilations (EDA) is used at ECMWF and elsewhere to represent random uncertainties in analyses and short-range forecasts of large NWP systems (Isaksen et al., 2010). It uses a Monte-Carlo approach to estimate the statistical characteristics of errors in analyses and short-range forecasts from the uncertainties in input parameters and the forecast model. This is done by running a finite number of independent cycling assimilation systems, in which observations and the forecast model are perturbed to generate different inputs for each member. The following aspects are perturbed in the EDA:

- Observations: These are perturbed according to the observation error covariances assigned in the assimilation system, assuming a Gaussian distribution with zero mean (Isaksen et al., 2010).
- Forecast model: Model error is represented by stochastic perturbations of the model physics (carried out using the Stochastically Perturbed Parametrised Tendency (SPPT) scheme, (Palmer et al., 2009)).
- Sea surface temperature (SSTs): These are perturbed according to climatological error structures.

Mathematically, the errors from the perturbed realisation of 4D-Var evolve with the same equations as the errors of the unperturbed version (see Appendix A for further mathematical details). A crucial measure of the EDA is the ensemble spread, i.e. the standard deviation of the ensemble members around the ensemble mean. If the characteristics of the perturbations in the ensemble members correctly represent the true errors, the spread of the ensemble will reflect the errors in analyses and forecasts.

At ECMWF, the EDA method has been operationally used since June 2010 (Isaksen et al., 2010; Bonavita et al., 2011) to fulfil two key requirements:

- Specification of background error statistics: The EDA is used to provide climatological as well as flow-dependent estimates of the statistical properties of the errors in the short-range forecasts (background) used in the high-resolution deterministic assimilation system. To capture flow-dependent aspects, an EDA is run alongside the high-resolution deterministic forecast system.
- Initialisation of the ensemble prediction system: Perturbations from the EDA are used together with Singular-Vector methods to initialise ECMWF's ensemble prediction system which provides probabilistic medium-range forecasts.

Operationally, 50 EDA members are currently used at ECMWF. The number of members used in the ensemble is a trade-off between computational affordability and reducing sampling noise in the background error estimates. For research-purposes EDAs with 10 members have been found to provide adequate estimates, at least for background error variances on larger scales.

2.2 Application of the EDA to simulate impact of future observations

The EDA method also provides a means of assessing the impact of potential future observations on analysis and short-range forecast error statistics. This is done by investigating how the spread of the

ensemble changes as we add new observations. The future new observations need to be simulated, for instance from high-resolution NWP analyses, whereas real observations can be used for all other observing systems. Expected error characteristics for the new observations are represented through applying appropriate perturbations in the EDA. When assessing changes in the observing system, a positive impact arises when the ensemble spread is reduced, indicating improved analysis/forecast error statistics.

The approach has been first developed by Tan et al. (2007) to simulate the expected impact of wind profile observations from Aeolus, and it has been subsequently applied by Harnisch et al. (2013) to study the expected benefits from further GNSS-RO observations. The latter study characterised the expected impact from a hypothetical constellation of GNSS-RO observations, and estimated the expected benefit as the number of observations increased, therefore providing input for determining a cost-effective target for the evolution of the GNSS-RO constellation. Tan et al. (2007) and Harnisch et al. (2013) both used relatively short experimentation periods, of the order of one month, which was motivated by relatively stable characteristics of the EDA spread.

To validate the EDA approach, and to establish the relationship between EDA spread reduction and more traditional measures of forecast impact, observing system experiments (OSEs) can be performed alongside EDA experiments for existing observations. For instance, Harnisch et al. (2013) performed a comparison of OSEs and EDA spread analyses using varying numbers of real GNSS-RO observations. In OSEs, the measure of observation impact is the reduction of the forecast error between assimilation experiments with and without selected observations. Harnisch et al. (2013) showed that the forecast error reductions from the OSEs were in good agreement with the reductions in the EDA spread when comparing equivalent OSE and EDA experiments with and without the selected set of observations. The comparison of results from OSEs and EDAs is sometimes referred to as a calibration step, and some scaling may be required in order to counter-act an under-dispersive ensemble (where the ensemble spread is smaller than the corresponding forecast error).

The EDA method has similar aims as the more traditional Observing System Simulation Experiments (OSSEs) (Arnold and Dey, 1986; Masutani et al., 2010). In these, simulated observations are generated from a "truth" - the "nature run" - and subsequently assimilated in an alternative forecast system (e.g. Masutani et al. (2007)). Harnisch et al. (2013) suggest that the two methods may be complementary while Tan et al. (2007) go further to argue that the EDA method is preferable. One clear disadvantage of the OSSE is that all the observations from both the existing and proposed new sources need be simulated, including their full error characteristics. This means that OSSEs can be problematic if errors are not adequately modelled for all observations. OSSEs are also computationally expensive, as long periods are required to establish statistically robust results. The EDA method can also be thought of as a 4D-Var theoretical error covariance/-information content study. Computing 4D covariance matrices directly is not practical due to the very large matrix dimensions required. However, the spread in the ensemble members provides an estimate of analysis/forecast error statistics of the 4D atmospheric state which includes the impact of a complex observing system and forecast model.

The EDA method is of course also not free from limitations either. Firstly, the method assumes that the perturbations applied in the EDA reflect the true error characteristics, but in practice these are both subject to their own uncertainties. Secondly, the EDA is a Monte Carlo method so the true values are only found in the limit of an infinite ensemble. This results in sampling errors from a finite ensemble size (Bonavita et al., 2011) and systematic errors can arise from incorrectly estimated error covariances (e.g. Cardinali et al. (2014)). By averaging over larger areas, such as hemispheric scales, small scale sampling errors can be reduced while keeping the large-scale changes in the EDA spread. Harnisch et al. (2013) also note that we can assume the systematic errors are similar across a set of experiments run with consistent settings and therefore the magnitudes of relative changes are unaffected.

3 Adaptation for the present study

The present study will use the EDA framework to study the expected impact from a future constellation of MW sounders on small satellites. In particular, it will provide input to the constellation design, for instance, to allow trade-offs regarding the number and type of orbits or the instrument design. The study has hence many similarities with work previously done in the context of GNSS-RO, which assessed the expected benefit from increasing the number of GNSS-RO observations (Harnisch et al., 2013) and trade-offs between the number of observations and different noise performance of the instrument (Healy, 2016).

Background to the present study is earlier work at ECMWF that investigated the impact of the existing MW sounders in OSEs and found continued positive impact from incrementally adding more MW sounders (Duncan and Bormann, 2020). They investigated the impact of adding 1, 3, 5, and 7 MW temperature and humidity sounders to a system that otherwise assimilated no MW sounding observations. The study was conducted over the 3 $\frac{1}{2}$ months 1 June - 15 September 2018, making use of a period with a good and stable coverage from heritage MW sounding instruments. The study showed that the largest impact is obtained from adding the first sounders, and even though the impact from adding further sounders is gradually smaller, significant benefits are still obtained from adding further instruments. The satellites and the temperature or humidity sounding instruments used in the 7-sounders experiment are summarised in table 1, and Fig. 1 provides a depiction of the temporal coverage provided. The combination of satellites was chosen to distribute temperature and humidity sounding capabilities as evenly as possible in a variety of orbits, within the constraints of the current observing systems. While other satellites such as FY-3C or Aqua are available, these do not provide both temperature and humidity sounding on the same platform and some alternative instruments are also limited in their usage e.g. due to loss of good data from all channels.

While Duncan and Bormann (2020) established the benefits of up to 7 MW temperature and humidity sounders using existing observations, the present study aims to characterise what further benefits could be obtained if further instruments were added using the EDA framework. We make use of a similar study period, hence allowing a direct link to the findings from real data in the OSEs. To bridge between the OSE and EDA framework, we first compare forecast error reductions seen in the OSEs with EDA spread reductions from EDA experimentation with real observations. EDA experiments with existing observations have been run for the no MW-sounder control experiment as well as the 7 MW-sounder experiment for the full 3 $\frac{1}{2}$ month period as part of the Duncan and Bormann (2020) study. The comparisons between the forecast error reduction and the EDA spread reductions for these experiments will be done in WP-2000 and reported at a later stage. They will allow us to gauge sub-optimalities in the performance of the EDA, arising from for example, imperfectly specified errors or a finite ensemble size.

The EDA configuration used throughout employs a $T_{Co}399$ (25km) resolution grid with 137 vertical levels and three inner loops at a resolution of TL95/TL159/TL255, and it comprises the control run and 10 perturbed ensemble members. This is a standard configuration of the EDA used at ECMWF for development testing and experimentation for future observing systems. For testing different scenarios of future instruments, EDA experiments will be conducted over 4-week periods, rather than the full 3 $\frac{1}{2}$ month period used in Duncan and Bormann (2020). This choice of length of experimentation period is motivated in section 3.1.

Throughout this project, we will focus mostly on the short-range EDA spread values at T+12 hours, as these are expected to exhibit the most robust signals. As the forecast length increases, model uncertainties increase, reducing the clarity of signals introduced by observation changes (Harnisch et al., 2013).

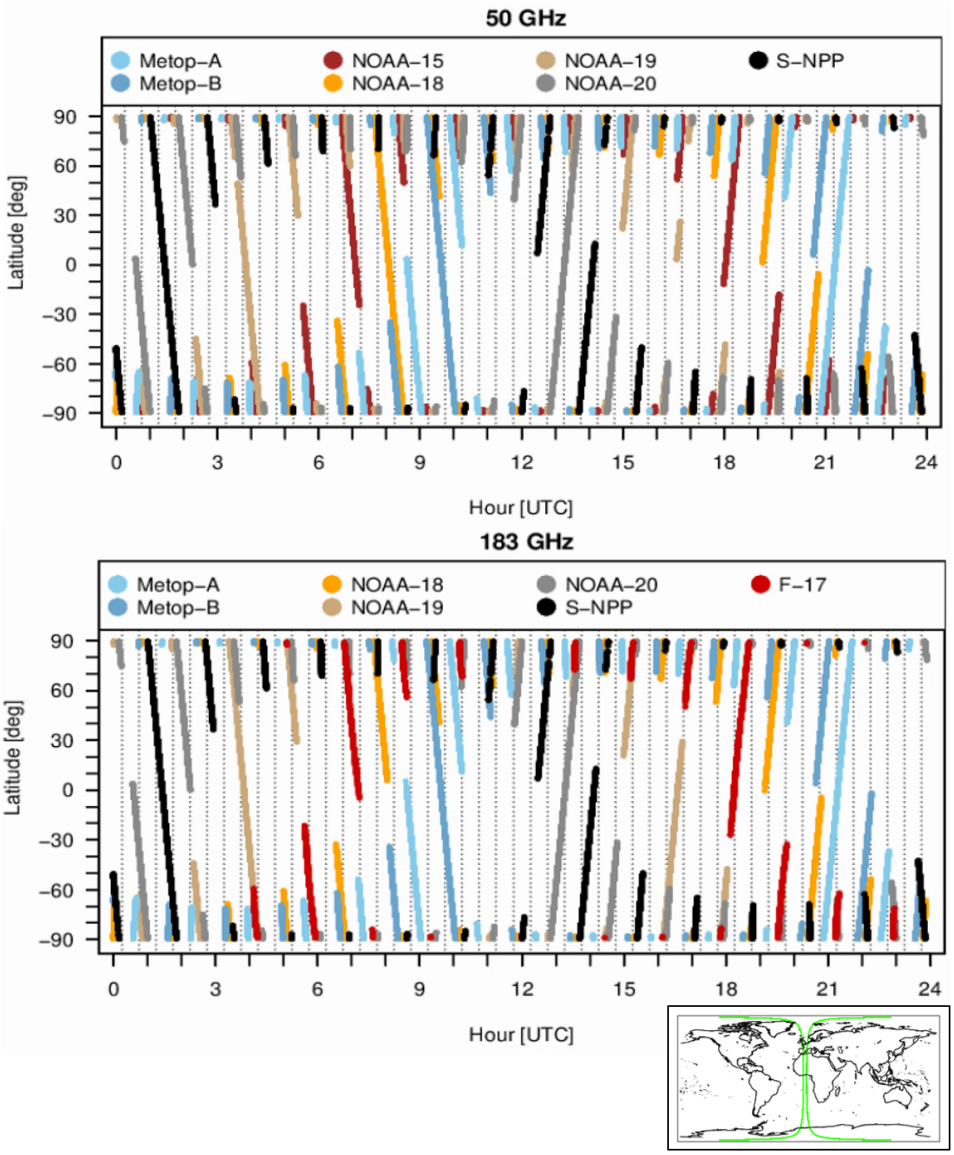

Figure 1: Temporal coverage on 15 July 2018 over 500 km stripe around 0° meridian (illustrated in insert, lower-right) for the 7 satellites assimilated in Duncan and Bormann (2020) study with MW data from temperature sounding (top) and humidity sounding (bottom) instruments.

Table 1: Details of satellites and their respective temperature and humidity sounding instruments included in the baseline EDA experiment to which different configurations of simulated small satellite observations will be added (ECT = approximate equator crossing time of descending node)

Satellite	Temperature sounding	Humidity sounding	ECT
Metop-A	AMSU-A	MHS	09:30
Metop-B	AMSU-A	MHS	09:30
NOAA-15	AMSU-A	-	06:30
DSMP F-19	-	SSMIS	06.30
NOAA-18	AMSU-A	MHS	08.00
NOAA-19	AMSU-A	MHS	04.00
NOAA-20	ATMS	ATMS	01:30
SNPP	ATMS	ATMS	01:30

3.1 Establishing the length of EDA study periods

The length of the study period used in the EDA experiments implies a trade-off between the number of scenarios that can be studied given computing resources and the statistical robustness of the results. When choosing an adequate length, two factors need to be considered: Firstly, when launching an EDA experiment, the system is initialised - cold started - with the same background fields. This means that a spin-up time is required before the signal in the EDA spread is reliable (Fisher et al., 2005). This spin-up time should not be included in the spread evaluation. Secondly, once the EDA has spun-up, the spread reductions will be partially affected by random fluctuations (sampling noise). The size of these will affect how long a period is required to achieve statistically robust results for a given signal in the spread reductions. If variations are small or the spread-reduction signal is large, shorter periods will be sufficient to establish a robust signal, whereas for smaller signals a longer period may be required.

Using the 3 $\frac{1}{2}$ month experiments already completed (control and seven satellite baseline), the EDA spread was computed for different variables and spanning the full atmosphere covered by the 137 model levels. Figures 2 and 3 show time series of the percentage difference in the EDA spread for the geopotential height and temperature in the troposphere and stratosphere and zonal wind speed and specific humidity in the troposphere only. These are also representative of global and southern hemisphere patterns. There is a clear spin-up period as predicted at the beginning with the values stabilising within a few days into the experiment period. After the spin-up period, model levels in the troposphere show a relatively stable signal. It is apparent from Figures 2 and 3 that excluding the first week of the experimentation period will successfully avoid the spin-up period of the EDA for the levels and variables of interest. These results are consistent with previous findings of Harnisch et al. (2013).

Next, we aim to establish what period to average our results over, in order to obtain statistically robust results. To do so, the 3 $\frac{1}{2}$ month time series was split into non-overlapping two-week chunks and the average spread was calculated for the whole experiment and for each of the shorter periods. This was repeated with three-, four- and five-week chunks. Figure 4 shows that results over a three-week period largely replicate the average reduction in spread seen over the 3 $\frac{1}{2}$ months, with variability of around 0.5-1 % for the quantities shown. This suggests that a three-week period would be sufficient to detect signals in spread reduction of this magnitude. This appears a useful detection threshold for the present study, given the expected signals in spread reduction. Longer periods increase robustness (not shown), though at the expense of greater computational cost. While the two-week periods also largely replicate

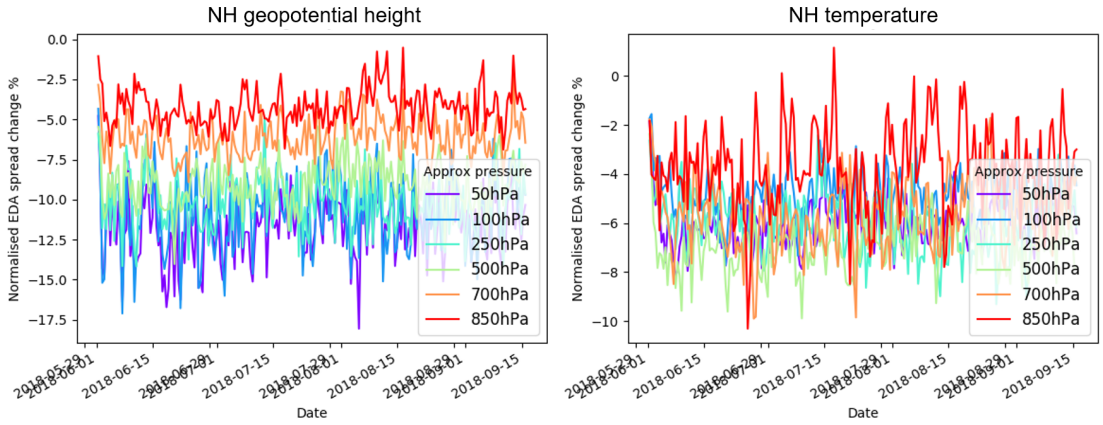

Figure 2: Time series for a selection of model levels (approximate pressures listed)showing the percentage difference in EDA spread (seven satellite baseline expt - control, normalised by the control) for geopotential height (left) and temperature (right) for each model cycle and averaged over the northern hemisphere (latitude $>$ 20N). Negative values indicate a reduction in spread, and therefore benefit, in the addition of MW sounding data.

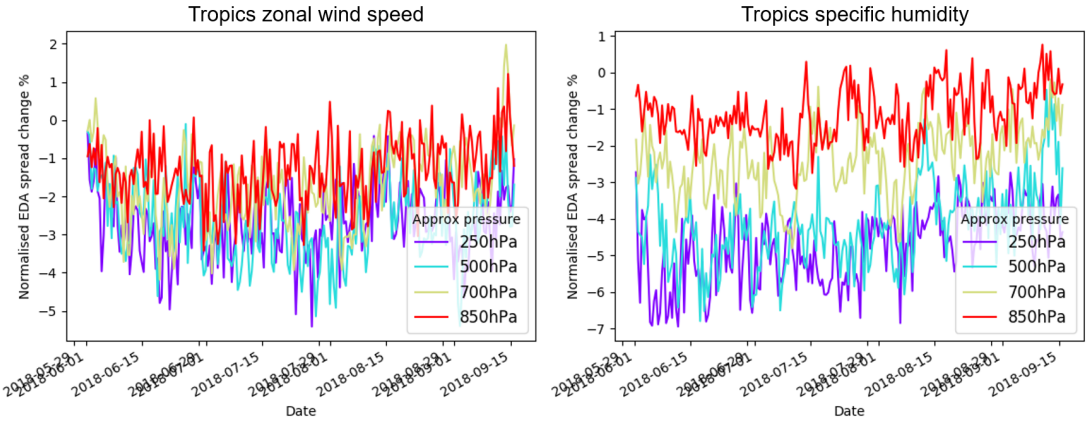

Figure 3: Time series for a selection of model levels (approximate pressures listed) showing the percentage difference in EDA spread (seven satellite baseline expt - control, normalised by the control) for zonal wind (left) and specific humidity (right) for each model cycle and averaged over the tropics (latitude $\pm$ 20N). Negative values indicate a reduction in spread, and therefore benefit, in the addition of MW sounding data.

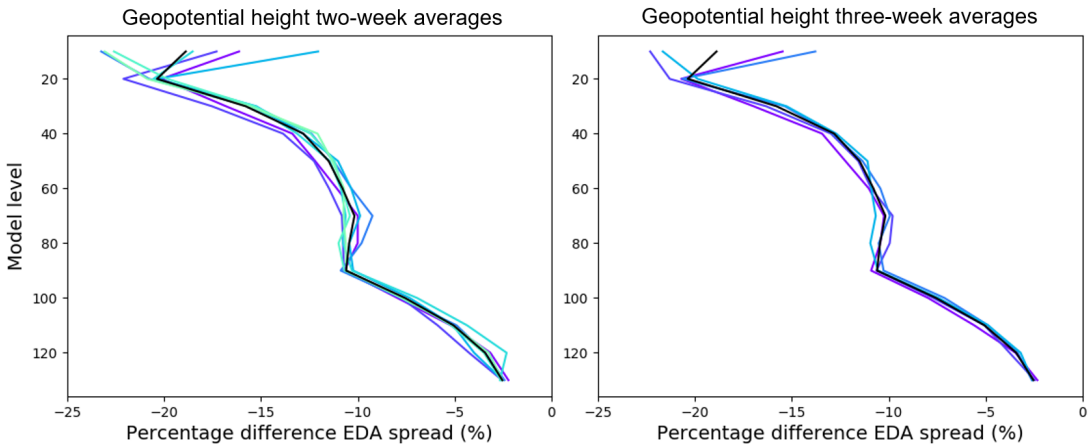

Figure 4: Profiles showing the average reduction in EDA spread in northern hemisphere geopotential height for non-overlapping two (left) and three (right) week periods within the experiment. The overall average reduction for the whole period is marked with the thick black line. Different coloured lines are otherwise used to differentiate each two/three-week complete profile.

the full signal (Fig. 4), the variability is somewhat larger, so smaller changes in the spread reduction may not be robustly detected.

In summary, based on this analysis a total of four weeks will be used for running each EDA experiment: the first week will be discarded during the spin-up period and the following three weeks will provide the spread statistics. The choice is consistent with findings in Harnisch et al. (2013).

3.2 Observation simulation and error representation

The new observations from the small satellite constellation will be simulated and assimilated in ECMWF's all-sky system. That is, observations will be used in clear, cloudy, and rainy situations, and they will be able to influence initial conditions through their impact on model clouds. This involves a fast radiative transfer model that is able to represent cloud effects, and the RTTOV-SCATT model is used for this purpose (Bauer et al., 2006). The all-sky approach has been shown to be particularly beneficial for humidity-sensitive observations, for which it significantly enhances the observation impact. One mechanism for this impact is the so-called 4D-Var tracing effect, that is, the ability of 4D-Var to infer wind information from the evolution of humidity or cloud structures. The all-sky approach has recently also been extended to MW temperature-sounding observations (Weston et al., 2019), and this will be adapted in the present study.

For each of the different configurations of small satellites, a set of observations will be simulated, as shown in the schematic in figure 5. The simulated small satellite data will be generated by first interpolating ECMWF NWP analysis fields in space and time to the locations of the observations. The radiative transfer model RTTOV-SCATT will then be used to convert the model information to corresponding satellite radiances. The spatial and temporal points for the observations will be taken from orbit simulations provided by ESA. Each scenario tested in an individual EDA experiment originates from a unique configuration of satellites defined e.g. by number, orbit type, channel set and performance characteristics. The inputs required from ESA are detailed in appendix B.

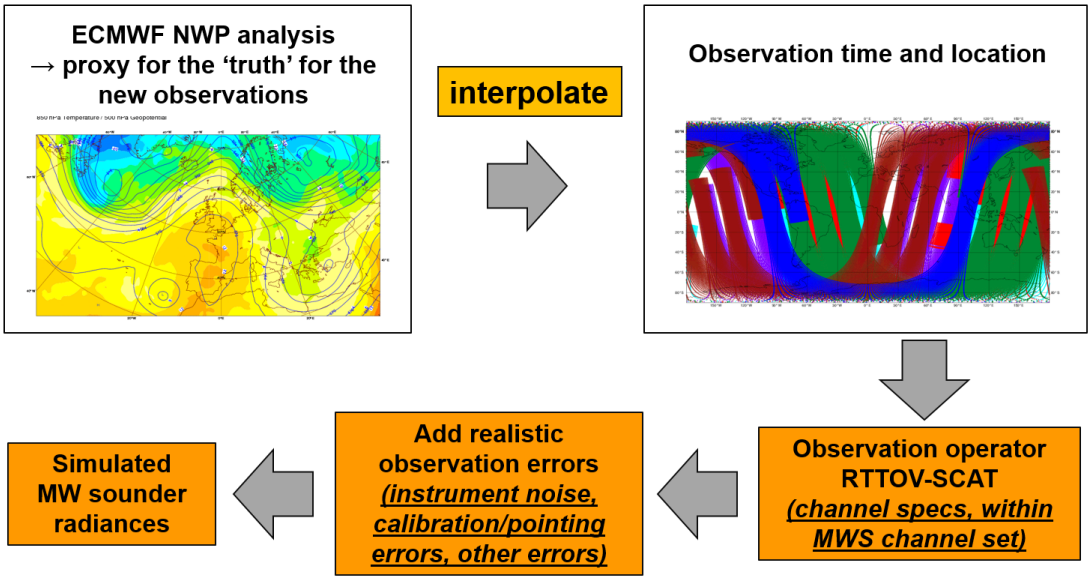

Figure 5: Simple schematic to illustrate the steps of generating simulated small satellite observations as input to EDA experiments

The specification of the uncertainties in the satellite data is an important aspect of the EDA - this is both in correctly generating the perturbations to the observations and also in the 4D-Var assimilation where it contributes to determining the weight of the observations in the final analysis. The observation error modelling will be based on the standard all-sky error model employed at ECMWF for all MW sounding observations assimilated in all-sky conditions, adapted from Geer et al. (2010). Observation errors are specified as a function of a cloud indicator, with lower values for clear-sky situations, rising to maximum values for cloudy scenes. The values for the clear-sky scenes will be set in line with instrument noise specifications provided by ESA for the new observations, with empirical adjustments derived from existing data to take into account other sources of error. The values for the cloudy scenes are dominated by representation error which is largely independent of the instrument specification for a given channel. Values will hence be adapted from currently used operational settings for heritage instruments. The cloud indicators used in the observation error model for MW sounding data are either liquid water path estimates derived from 23.8 and 31 GHz channels (Grody et al., 2001), or a suitable scattering index (Bennartz et al., 2002). This choice will need to be revisited for the new observations from small satellites, as some of the lower-frequency channels may not be available. In this case, the difference between observations and clear-sky simulations for the lowest-peaking 50 GHz channel may offer a suitable alternative. This aspect will be considered further in WP-2000.

Error contributions due to differences in spatial representativeness between observations and model fields are presently not explicitly modelled in the ECMWF system, though they are implicit in the empirically derived observation error setting. Different field-of-view sizes of the new MW data will lead to differences in the size of spatial representativeness errors. While such effects could be included in the observation error modelling for the new observations, it should be noted that explicit modelling of representation error is a field of active research, and any attempts employed in the present study will necessarily need to be ad-hoc.

Ideally, systematic biases in the small satellite data would be of similar structure to those already en-

countered in current MW data. In this case, the variational bias correction scheme which is already successfully employed at ECMWF to remove such biases should also be effective for small satellite data. However, if these biases have different characteristics new ways of accounting for them would have to be developed. The question of how effectively these biases can be removed is not important to the goals of this study considering the fundamental design of the future constellation is unlikely to be impacted.

3.3 Proposed scenarios

In the following we consider the scenarios to be addressed in EDA experiments. We envisage 10 scenarios, that is, a given realisation of a constellation of small satellites with a particular instrument specification (including the scanning pattern, channel complement, noise performance). Each of these scenarios will require a separate EDA, so given resource limitations prioritisation of scenarios is needed.

The scenarios proposed here are addressing specific scientific or technological questions, following on from recommendations made at the expert meeting, as outlined below. The separation of humidity sounding channels from humidity plus temperature configurations will help to establish where the majority of forecast impact can be attained. This can be through the better temporal sampling of evolving humidity features, which in turn also brings dynamical information. Alternatively, the additional temperature information, which helps to reduce the effective noise through repetitive measurement, may provide a crucial advantage. From a technological perspective, the testing of the higher frequency humidity channels alone and possibly with scenario that includes degraded noise values could also be useful to suggest whether there is potential in an even smaller platform cubesat mission.

A recent meeting of experts provided recommendations around the channel selection for a potential MW sounding instrument for a new small satellite constellations (EUMETSAT, 2019), complementing already planned larger missions with fully-specified instruments. Starting from the channel set from EPS-SG MicroWave Sounder (MWS), they concluded that humidity sounding channels around the 183 GHz line were considered the highest priority, followed closely by tropospheric and lower stratospheric temperature-sounding channels in the 50 GHz band, and accompanied with a selection of window channels around 89, 165, and 229 GHz.

The motivation for employing a set of channels is different for the humidity and temperature-sounding sets. One motivation for the humidity-sounding channels is that higher temporal sampling would better capture the shorter timescale humidity and cloud features. This is expected to further aid the exploitation of the tracing effect of 4D-Var which allows wind information to be inferred from observations sensitive to humidity and clouds. The 183 GHz channels are also more easily accommodated on a small satellite due to the smaller antenna size required to achieve acceptable field-of-view sizes. The motivation for temperature-sounding channels is further reduction of the effective noise through providing more observations. In today's state-of-the-art NWP systems, the random errors of the model background in the troposphere are typically of the order of a tenth of a degree Kelvin. As it becomes difficult to achieve comparable or lower levels of uncertainty in MW observations, repetitive measurement can effectively reduce the noise.

To optimise the design and use of a MW sensor on small satellites, the expert meeting recommended studies to further refine the selection of channel sets, as well as the number and types of orbits used for the small satellites. The following proposed scenarios therefore span different numbers of additional orbits, to allow trade-off studies in this direction, as well as address the question of the relative benefit of humidity and temperature sounding capabilities.

Selecting different configurations of orbits can also give insight for example into the advantages of better

sampling the storm track regions using lower inclination orbits. It was highlighted earlier with figure 1 that the tropics and mid-latitudes show sparser coverage than polar regions. The use of the all sky framework in particular will allow use of the small satellite observations in high impact areas where the presence of cloud can be challenging for other components of the current observing system such as the infrared sounders. A higher temporal sampling rate from additional lower inclination orbits compared to use of polar orbits only may help to more accurately capture faster evolving mid-latitude and tropical features.

The proposed scenarios are provided in table 2 where there are four key themes that have motivated the selection:

1. How many orbits? We have not yet detected a saturation of positive impact with the addition of MW sounding data. How much extra benefit can we continue to achieve while still being cost effective? Comparing results from scenarios 1-4 or 5-8 will allow to answer these questions. A realistic range of the number of orbits will need to be defined with ESA; the present numbers are indicative only.

2. Humidity or temperature sounding? Comparing the scenarios 1-8 investigate the added benefit of the temperature-sounding capability as the number of observations is increased. This will address whether the better temporal sampling for humidity is the dominant mechanism for achieving better forecast impact, or whether a combination of channels is required to optimise system performance.

3. What types of orbit to use? Small satellites provide an opportunity to greatly increase coverage of the tropics and storm tracks in the mid-latitudes where the higher temporal sampling could also be very beneficial in the development of higher impact weather. Polar orbits would naturally cover these areas in addition to the polar regions but a larger constellation would be required. Lower inclination or a mixture of the orbit types would allow denser coverage while allowing the complementary large satellite system to still cover much of the poles. Scenarios 9a and 10a could offer alternative orbit configurations, possibly conducted after the results of scenarios 1-8 provide initial guidance on what constitutes a useful trade-off.

4. What is the influence of instrument noise performance? As an alternative to scenarios 9a and 10a, scenarios 9b and 10b could consider different levels of noise performance for the selected channels, hence providing trade-off guidance for further this design aspect.

The above scenarios are intended to be added to the 7 MW-sounder baseline used in Duncan and Bormann (2020). This means that combined with the results for 1, 3, 5, and 7 sounders used in Duncan and Bormann (2020), the present study will enable the assessment of the expected forecast impact of up to 31 MW sounding instruments. While doing so, we accept that our chosen baseline number of orbits may not reflect the baseline to which a future constellation will be added, as instruments are decommissioned or fail. However, the choice allows to concentrate on the scenarios which investigate capabilities not yet available, which is the primary aim of the study. In any case, by providing results for constellations of 1, 3, 5, and 7 heritage sounders, the study of Duncan and Bormann (2020) implicitly characterises the benefit expected when fewer than 7 instruments are available.

Note that this is an initial proposal and that further iteration with ESA is expected regarding, for example, practical concerns of such constellations before finalising. The exact orbit placement will be subject to further study by ESA or its contractors. Ideally, the spacing of the small satellites would avoid duplication as much as possible with the large satellites. The geo-location accuracy is expected to be comparable to the specifications for MWS rather than being more limited by the compact technology. Consequently, the scenarios we have chosen do not investigate impacts from inaccuracies in this aspect at this time.

Table 2: Proposed list of scenarios to test in EDA experiments. Humidity channels relate to a group around 183GHz while temperature sounding relates to channels around 55GHz (window channels at 89, 165, and 229 GHz are expected to be available in either case). Low inclination is suggested as around 65° and orbital planes for each scenario are suggested to be evenly distributed. "Nominal" instrument performance refers to, for instance, instrument noise performance in line with expectations from heritage instruments or MWS, whereas "degraded noise" refers to an instrument design in which the noise performance is compromised compared to heritage instruments or MWS.

Expt no.	Temperature (T) or Humidity (H)?	Number of satellites	Orbit type	Instrument performance
1	H	3	Polar	nominal
2	H	6	Polar	nominal
3	H	12	Polar	nominal
4	H	24	Polar	nominal
5	T + H	3	Polar	nominal
6	T + H	6	Polar	nominal
7	T + H	12	Polar	nominal
8	T + H	24	Polar	nominal
9a	H	tbd	Mix of polar/low inclination	nominal
10a	T + H	tbd	Mix of polar/low inclination	nominal
9b	H	tbd	Polar	degraded noise
10b	T + H	tbd	Polar	degraded noise

4 Concluding remarks

This report elaborates the conceptual basis of the present study, aimed at characterising the forecast impact that can be expected from MW sounding instruments on-board a constellation of small satellites that complements a back-bone constellation with fully specified sounding capabilities. The EDA framework used to simulate the expected impact has been described, including the adaptations that will be made for the present study. The expected impact will be assessed on the basis of reductions in the spread of the EDA, and we established that an experimentation period of 4 weeks is expected to be sufficient to robustly characterise spread reductions of 0.5-1 % for most areas and variables of interest. A range of scenarios has been proposed to study key questions relating to orbit and instrument design, intended as a starting point for further discussions with ESA on final scenario definitions. Details of input required from ESA for the constellation simulation are given in Appendix B.

The next step in the study will compare the forecast impact found in OSEs with existing sensors to the reduction in spread seen in equivalent EDA experiments, to link the results of the present study to already existing OSEs with the present MW sounding constellation. This will form part of WP-2000, which will also more closely consider necessary adaptations of the observation error modelling outlined in section 3.2.

Acknowledgements

The authors would like to thank Stephen English for his advice and comments on an earlier draft of the report and Elias Hòlm for discussion on aspects of the EDA.

Appendix A Theoretical outline of EDA technique

Full discussion of the EDA method can be found in publications such as Isaksen et al. (2010) and Žagar et al. (2005). However, to support the techniques that will be used in this study a brief description is presented here to outline the mathematical steps that confirm that use of the EDA leads to forecast and analysis error statistics.

Consider a linear system which uses a linear forecast model, **M**, and a linear observation operator to move from model space to observation space, **H**. The data assimilation equation that updates the model state can be written as:

$$\mathbf{x}_t^a = \mathbf{x}_t^b + \mathbf{K}_t(\mathbf{y}_t - \mathbf{H}_t\mathbf{x}_t^b) \tag{1}$$

$$\mathbf{x}_{t+1}^b = \mathbf{M}_t\mathbf{x}_t^a \tag{2}$$

Where t is the analysis time, $\mathbf{x}^a$ is the model analysis state, $\mathbf{x}^b$ is the model background state, $\mathbf{y}^t$ is the vector of observations and $\mathbf{K}$ is the gain matrix.

Assuming independent background, observation and model errors, represented by error covariance matrices $\mathbf{P}^b$, $\mathbf{R}$ and $\mathbf{Q}$ respectively, the analysis error covariance matrix $\mathbf{P}^a$ can be written as:

$$\mathbf{P}_t^a = (\mathbf{I} - \mathbf{K}_t\mathbf{H}_t)\mathbf{P}_t^b(\mathbf{I} - \mathbf{K}_t\mathbf{H}_t)^T + \mathbf{K}_t\mathbf{R}_t\mathbf{K}_t^T \tag{3}$$

$$\mathbf{P}_{t+1}^b = \mathbf{M}_t\mathbf{P}_t^a\mathbf{M}_t^T + \mathbf{Q}_t \tag{4}$$

In the EDA technique, the data assimilation system is run with perturbed observations and forecast model where values have been generated randomly from Gaussian distributions with zero mean and standard deviations of the respective error covariances. This means that perturbations for the observations and model can be written as $\zeta \sim \mathcal{N}(0, \mathbf{R})$ and $\eta \sim \mathcal{N}(0, \mathbf{Q})$ respectively. By updating equations 1 and 2 to include the perturbations we have:

$$\tilde{\mathbf{x}}_t^a = \tilde{\mathbf{x}}_t^b + \mathbf{K}_t(\mathbf{y}_t + \zeta - \mathbf{H}_t\tilde{\mathbf{x}}_t^b) \tag{5}$$

$$\tilde{\mathbf{x}}_{t+1}^b = \mathbf{M}_t\tilde{\mathbf{x}}_t^a + \eta \tag{6}$$

Where $\tilde{\mathbf{x}}^b$ and $\tilde{\mathbf{x}}^a$ are now the perturbed model background and analysis states. Calculating the differences between the perturbed and unperturbed states (equation 1 - 5) shows that the perturbations actually evolve with the similar updates as the control:

$$\varepsilon_t^a = \tilde{\mathbf{x}}_t^a - \mathbf{x}_t^a = \varepsilon_t^b + \mathbf{K}_t(\zeta - \mathbf{H}_t\varepsilon_t^b) \tag{7}$$

$$\varepsilon_{t+1}^b = \tilde{\mathbf{x}}_{t+1}^b - \mathbf{x}_{t+1}^b = \mathbf{M}_t\varepsilon_t^a + \eta \tag{8}$$

The corresponding error covariances of the perturbations become:

$$\overline{\varepsilon_t^a(\varepsilon_t^a)^T} = (\mathbf{I}-\mathbf{K}_t\mathbf{H}_t)\overline{\varepsilon_t^b(\varepsilon_t^b)^T}(\mathbf{I}-\mathbf{K}_t\mathbf{H}_t)^T + \mathbf{K}_t\mathbf{R}_t\mathbf{K}_t^T \tag{9}$$

$$\overline{\varepsilon_{t+1}^b(\varepsilon_{t+1}^b)^T} = \mathbf{M}_t\overline{\varepsilon_t^a(\varepsilon_t^a)^T}\mathbf{M}_t^T + \mathbf{Q}_t \tag{10}$$

By comparing equation 9 with 3 and equation 10 with 4 it is possible to see that $\overline{\varepsilon_{t+1}^b(\varepsilon_{t+1}^b)^T} = \mathbf{P}_{t+1}^b$ and $\overline{\varepsilon_t^a(\varepsilon_t^a)^T} = \mathbf{P}_t^a$ and hence the error statistics of the analysis/forecast system can be estimated by the perturbed members from the EDA.

In this study we consider only the error variances rather than the full covariance matrix which leads to the EDA spread which is defined as the standard deviation of ensemble members around the ensemble mean:

$$s = \sqrt{\frac{1}{D}\sum_{d=1}^{D}\left[\frac{1}{N-1}\sum_{n=1}^{N}(\mathbf{x_n}-\bar{\mathbf{x}})^2\right]_d} \tag{11}$$

Where D is the required time period e.g. the number of model cycles, N is the size of the ensemble (10 members for this study), $\mathbf{x_n}$ is the model state from a single ensemble member and $\bar{\mathbf{x}}$ is the ensemble mean.

Appendix B ESA inputs for simulated data

Each scenario tested in an individual EDA experiment originates from a unique configuration of satellites defined e.g. by number, orbit type, channel set and performance characteristics. For each scenario ESA will need to provide files containing a unique combination of the variables below, simulated for a given orbit configuration and instrument sampling pattern. An estimate of the likely precision required is also indicated where appropriate (dp = decimal places). Initial input files that establish for example the file type and format, but not necessarily the full final content, are required by 1st April 2021 to allow technical development to proceed at ECMWF. Final input files that relate to the ultimately agreed set of scenarios will be required by 1st October 2021.

For each field of view for the constellation:
Latitude (5 dp)
Longitude (5 dp)
Time (seconds to 3 dp)
Field of view number (indicating the position across the scan)
Scan line number (identifying each separate scanline of one complete orbit of a satellite)
Satellite Zenith Angle (degrees, 2 dp)
Satellite Azimuth Angle (degrees, 2 dp)
(All the above assumed the same for all channels. dp = decimal places)

For each channel (using MWS channels as reference):
Estimate of instrument noise (equivalent of warm calibration target estimate) (2 dp)

Optional error information
After further iteration, if another type of error needs to be considered (e.g., geolocation, orbital variations in calibration stability), a model for this error will need to be provided. This could be provided in the form of prototype code and would aim to follow a relatively simple implementation.

File format
The most convenient format of these files is anticipated to be simple text files. Data split into six hourly chunks would be easiest as this replicates the current structure in the ECMWF system. Each six-hour period should be centred on 00, 06, 12 and 18Z i.e. in the 00Z file, observations fall between 21Z-03Z. Files will be required for a length of four weeks corresponding to an experiment period running 1st - 28th June 2018 inclusive. Some of the scenarios proposed will almost certainly share the same orbit parameters (e.g. but with different channel selection). Rather than a set of files for each scenario which would involve some duplication, we suggest producing a set for each unique orbit required across all the scenarios. We can then more flexibly use a sub-selection of these to generate the required combination of orbits and channels for each scenario. Note that if the alternative option of a set per scenario is used, channel numbers and unique identification for each satellite if multiple satellites are within the same file will be required (e.g. simply by number 1, 2, ...).

References

Arnold, C. P., J., Dey, C. H., 1986. Observing-Systems Simulation Experiments: Past, Present, and Future. Bulletin of the American Meteorological Society 67 (6), 687–695.

Bauer, P., Moreau, E., Chevallier, F., O'Keeffe, U., 2006. Multiple-scattering microwave radiative transfer for data assimilation applications. Quart. J. Roy. Meteorol. Soc., 1259–1281.

Bennartz, R., Thoss, A., Dybbroe, A., Michelson, D., 2002. Precipitation analysis using the Advanced Microwave Sounding Unit in support of nowcasting applications. Met. Apps, 177–189.

Bonavita, M., Raynaud, L., Isaksen, L., 2011. Estimating background-error variances with the ECMWF Ensemble of Data Assimilations system: some effects of ensemble size and day-to-day variability. Quart. J. Roy. Meteorol. Soc., 423434.

Bormann, N., Lawrence, H., Farnan, J., 2019. Global observing system experiments in the ECMWF assimilation system. ECMWF Technical Memorandum No.839.

Cardinali, C., Žagar, N., Radnoti, G., Buizza, R., 2014. Representing model error in ensemble data assimilation. ECMWF Technical Memorandum.

Duncan, D. I., Bormann, N., 2020. On the Addition of Microwave Sounders and NWP Skill, Including Assessment of FY-3D Sounders. EUMETSAT/ECMWF Fellowship Programme Research Report No.55.

EUMETSAT, 2019. Considerations on user requirements for additional mini-Microwave sounders. EUM/STG/75/19/DOC/18.

Fisher, M., Leutbecher, M., Kelly, G., 2005. On the equivalence between Kalman smoothing and weak-constraint four-dimensional variational data assimilation. Quart. J. Roy. Meteor. Soc., 32353246.

Geer, A., Bauer, P., Lopez, P., 2010. Direct 4D-Var assimilation of all-sky radiances. Part II: Assessment. ECMWF Technical Memorandum No.619.

Grody, N., Zhao, J., Ferraro, R., Weng, F., , Boers, R., 2001. Determination of precipitable water and cloud liquid water over oceans from the NOAA 15 advanced microwave sounding unit. J. Geophys. Res., 29432953.

Harnisch, F., Healy, S. B., Bauer, P., English, S. J., 2013. Scaling of GNSS Radio Occultation Impact with Observation Number Using an Ensemble of Data Assimilations. Mon. Wea. Rev. 141, 43954413.

Healy, S. B., November 2016. Final report of esa contract 4000116920/16/nl/ff/gp Using an Ensemble of Data Assimilations to assess the impact of GNSS Radio Occultations from ORORO nano-satellites. ESA Contract 4000116920/16/NL/FF/gp Final Report (unpublished), ECMWF, Reading, UK.

Isaksen, L., Bonavita, M., Buizza, R., Fisher, M., Haseler, J., Leutbecher, M., Raynaud, L., 12 2010. Ensemble of data assimilations at ECMWF, 45.
URL https://www.ecmwf.int/node/10125

Masutani, M., Andersson, E., Terry, J., Reale, O., Jusem, J., Riishøjgaard, L., Schlatter, T., Stoffelen, A., Woollen, J., Lord, S., Tóth, Z., Song, Y., Kleist, D., Xie, Y., Prive, N., Liu, E., Sun, H., Emmitt, D., Boukabara, S.-A., 2007. Progress in joint osses a new nature run and international collaboration. AMS preprint volume for 18th conference on Numerical Weather Prediction, Parkcity UT. 25-29 June, 2007.

Masutani, M., Schlatter, T., Errico, R., Stoffelen, A., Andersson, E., Lahoz, W., Woollen, J., Emmitt, G., Riishøjgaard, L.-P., Lord, S., 01 2010. Data Assimilation: Making sense of observations, Observing System Simulation Experiments.

Palmer, T., Buizza, R., Doblas-Reyes, F., Jung, T., Leutbecher, M., Shutts, G., Steinheimer, M., Weisheimer, A., 2009. Stochastic parametrization and model uncertainty. ECMWF RD Tech. Memo., 42.

Tan, D. G. H., Andersson, E., Fisher, M., Isaksen, L., 2007. Observing-system impact assessment using a data assimilation ensemble technique: Application to the ADM-Aeolus wind profiling mission. Quart. J. Roy. Meteor. Soc. 133, 381390.

Žagar, N., Andersson, E., Fisher, M., 2005. Balanced tropical data assimilation based on a study of equatorial waves in ECMWF short-range forecast errors. Quart. J. Roy. Meteorol. Soc. 131, 987–1011.

Weston, P., Geer, A., Bormann, N., 2019. Investigations into the assimilation of AMSU-A in the presence of cloud and precipitation. EUMETSAT/ECMWF Fellowship Programme Research Report No.50.